

# Examination of temperature-induced ‘gel-sol’ transformation of $\alpha$ -actinin/cross-linked actin networks by static light scattering

Wolfgang H. Goldman\*, Zeno Guttenberg

Surgery Research Laboratories, Massachusetts General Hospital, Harvard Medical School, Building 149, 13th Street, Charlestown, MA 02129, USA

Received 7 March 1998

**Abstract** We studied the gel-sol transformation of F-actin/ $\alpha$ -actinin solutions. Cross-linking of actin filaments by  $\alpha$ -actinin shows a temperature-dependent increase in light scatter signal,  $(I)T$ . Higher F-actin/ $\alpha$ -actinin molar ratios,  $r_{A\alpha}$  as well as increases in F-actin concentration,  $[A]$ , and reduction of actin filament lengths,  $r_{AG}$ , augment the maximal light intensity,  $I$  and shift the gel-sol transition point,  $T_g$  to higher temperatures. This behavior is interpreted in terms of the model developed by Tempel, M., Isenberg, G. and Sackmann, E. (1996) (Physical Review E 54, 1802–1810) based on the percolation theory. Using the temperature-dependent binding model of this theory allows instant prediction of the equilibrium constant,  $K$  for F-actin/ $\alpha$ -actinin solutions at temperatures  $T < T_g$ .

© 1998 Federation of European Biochemical Societies.

**Key words:** Actin;  $\alpha$ -Actinin; Binding kinetics; Light scattering

## 1. Introduction

$\alpha$ -Actinin belongs to the family of actin cross-linking proteins and importantly to the group of bundling proteins that includes fibrin or villin [1,2]. Actin bundling proteins influence the parallel array of filaments that macroscopically change gels from isotropic to anisotropic. At physiological conditions,  $\alpha$ -actinin behaves like a rod-like, dumbbell-shaped homodimer that has a length depending on the isoform of 35–47 nm, a width of 2–3 nm, and a molecular mass of  $\sim 100\,000$  [3]. Since the formation of dimers is antiparallel it allows binding of actin filaments at opposite ends, cross-linking, and tight network formation.

The influence of  $\alpha$ -actinin on the physical properties of actin networks has been evaluated by various methods [4–7]. Our group as well as others have previously been interested in determining the binding parameters for actin/ $\alpha$ -actinin solutions at different temperatures [8–10] and have observed with increasing temperature a decrease in the equilibrium constant,  $K$ . Recently, Tempel et al. [11], using a magnetically driven

rotating disc rheometer, examined the effect temperature has on the viscoelastic and structural properties of actin networks composed of semiflexible actin filaments cross-linked by  $\alpha$ -actinin. These authors reported that the degree of cross-linking can be regulated in a reversible way by varying the temperature throughout the association-dissociation equilibrium of the F-actin/ $\alpha$ -actinin system. Three types of network structures were defined with reference to the gel-sol transition point,  $T_g$ : (i) homogeneous gel at  $T > T_g$ , (ii) microscopic segregation (microgel) at  $T < T_g$  and (iii) macroscopic segregation (bundle formation) at  $T \leq 10^\circ\text{C}$ . Thus, the gel point varied by a factor of 2 when the molar ratio of  $\alpha$ -actinin to actin,  $r_{A\alpha}$  was changed by a factor of 5. The observed ‘gel-sol’ transformation was explained in terms of a percolation model for the shear elastic constant,  $G_{(N)}'$  at  $T < T_g$ .

In the present study, we used the spectrofluorimeter measuring changes in light scatter signal,  $\Delta I$  of F-actin to  $\alpha$ -actinin solutions at various molar ratios,  $r_{A\alpha}$ . We obtained similar curve profiles and changes in  $T_g$  that depend on temperature as described by Tempel et al. [11]. Using their binding model of the percolation theory, which allows the determination of the equilibrium constant  $K$  at temperatures  $T < T_g$ , we confirm its validity by stopped flow measurements.

## 2. Materials and methods

### 2.1. Protein preparations

$\alpha$ -Actinin was isolated from turkey gizzard by the method of [12]. The purity of  $\alpha$ -actinin was determined, using 7.5% sodium dodecyl sulfate-polyacrylamide gel electrophoresis, following Laemmli [13]. The concentration of purified  $\alpha$ -actinin was measured by UV spectroscopy, using an extinction coefficient of  $97\,000\text{ M}^{-1}\text{ cm}^{-1}$  at 278 nm.

Actin was prepared according to the procedure of Spudich and Watt [14] from acetone powder obtained from rabbit back muscle. The protein concentration was determined using  $E_{290\text{nm}} = 26\,460\text{ M}^{-1}\text{ cm}^{-1}$ . G-actin was stored in G-buffer: 2 mM Tris/HCl, pH 7.5; 0.2 mM  $\text{CaCl}_2$ , 0.5 mM ATP, 0.2 mM DTT and 0.005%  $\text{NaN}_3$ , either kept on ice for less than two days or rapidly frozen using liquid nitrogen, kept at  $-80^\circ\text{C}$ , and thawed right before use. For the light scatter studies, all proteins were added at the same time to F-buffer: 2 mM imidazole, pH 7.4; 50 mM KCl, 2 mM  $\text{MgCl}_2$ , 1 mM EGTA, 0.2 mM  $\text{CaCl}_2$ , 1 mM ATP; and actin was polymerized overnight at  $4^\circ\text{C}$  prior to experimentation.

Gelsolin was purified from bovine plasma serum using the procedure described by Cooper et al. [15]. The concentration was determined by the Bradford method [16], with BSA as standard.

### 2.2. Static light scattering

Light scattering (LS) was carried out in a Perkin-Elmer LS-5B spectrofluorimeter. The temperature of the cell-holder was controlled thermostatically by an external water bath ( $\pm 0.1^\circ\text{C}$ ), and measured electronically by a sensor in the cell. A 1 ml four sided quartz cuvette of 1 cm path length was used for these measurements. Proteins were added and gently mixed by hand to prevent the formation of air bubbles. The light scatter signal was recorded at 350 nm and at  $90^\circ$

\*Corresponding author. Fax: +1 (617) 726-5669.  
E-mail: goldman@helix.mgh.harvard.edu

**Abbreviations:**  $T_g$ , temperature-dependent gel-sol transition point;  $\Delta I$ , change in light scatter intensity;  $K$ , equilibrium constant; UV, ultraviolet light;  $p_\alpha$ , portion of bound  $\alpha$ -actinin to actin;  $\Delta H$ , heat of association;  $K_0$ , proportionality constant;  $R$ , gas constant;  $T$ , absolute temperature (Kelvin);  $(I)T$ , temperature-dependent light scatter intensity;  $I=I_s/I_o$ , light scatter intensity equals the ratio of incident/reflected light;  $[\alpha]$ ,  $\alpha$ -actinin concentration;  $[A]$ , F-actin concentration;  $[C]$ ,  $\alpha$ -actinin/F-actin complex;  $p_\alpha(T)$ , temperature-dependent portion of bound  $\alpha$ -actinin to actin;  $J(t)$ , time-dependent creep;  $r_{A\alpha}$ , ratio of F-actin to  $\alpha$ -actinin;  $r_{AG}$ , ratio of F-actin to gelsolin

angle to the incident light with a band pass width of 1 nm. Data were collected on a PC computer and later transferred to an Apple Macintosh IIfx computer and analyzed on a commercially available program (Igor Pro 3).

Prior to measurements, the samples were equilibrated at 4°C for 40 min. During measurements, the temperature was linearly increased between 6°C and 25°C at a rate of 2°C/min (Fig. 1). To prevent condensation a constant flow of N<sub>2</sub> was applied.

The stopped flow apparatus described in detail by Goldmann et al. [10] was applied to measure the binding parameters of F-actin/ $\alpha$ -actinin solutions at various temperatures.

### 2.3. Theoretical basis of temperature-dependent binding

In our analysis, we used the model developed by Tempel et al. [11] which is based on the percolation theory [17]. Here, these authors have provided a qualitative description of the 'gel-sol' transition of an actin/ $\alpha$ -actinin solution, with temperature in considering the following equilibria:



$$K = \frac{[C]}{[A][\alpha]}, \quad (1b)$$

where  $\alpha$  =  $\alpha$ -actinin,  $A$  = F-actin,  $C$  = complex of  $\alpha$ -actinin and F-actin,  $K$  = equilibrium constant, and the brackets indicate protein concentrations. The portion of bound  $\alpha$ -actinin to F-actin,  $p_\alpha$ , is defined as follows:

$$p_\alpha = \frac{[C]}{[C] + [\alpha]} = \frac{[A]K}{[A]K + 1} \quad (2)$$

and for  $K$ , the following temperature-dependent behavior is assumed:

$$K = K_0 \exp\left(\frac{\Delta H}{RT}\right), \quad (3)$$

where  $\Delta H$  = heat of association,  $K_0$  = proportionality constant,  $R$  = gas constant, and  $T$  = absolute temperature (Kelvin). Inserting the terms of Eq. 3 in Eq. 2 and taking into consideration that two binding events of the  $\alpha$ -actinin homodimer are necessary to cross-link actin filaments, yields the following term:

$$p(T) = \frac{1}{2} p_\alpha(T) = \frac{1}{2} \frac{[A]K_0 \exp(\Delta H/RT)}{[A]K_0 \exp(\Delta H/RT) + 1}. \quad (4)$$

The percolation theory requires the existence of clusters, and since the intensity of scattered light is the mean value of all clusters, we assumed for quantitative analyses of the intensity signals,  $I(T)$ , the following temperature-dependent relation:

$$I(T) \propto p(T). \quad (5)$$

Note: Percolation models the mechanical properties of random elastic (here: actin) networks. Above a critical temperature and concentration (here:  $\alpha$ -actinin) the system develops macroscopic elastic properties in a continuous manner, which are reflected by  $G'_{(N)}$  in the rheometer. Static light scattering measures the intensity ( $I$ ) of a system (here: actin/ $\alpha$ -actinin solution) with temperature, which is the sum of all the reflected light i.e. the scatter intensity ( $I$ ) is proportional to increasing local bundling of actin filaments by  $\alpha$ -actinin. For further reading cf. [18,19].

## 3. Results

A prerequisite for applying the kinetic model (Eq. 3) of the percolation theory is that a solution has reached *steady state* at every temperature. Our first experiments were, therefore, directed at elucidating the optimal heating time. We used static light scattering intensity  $I = I_s/I_0$  to detect changes at a 90° angle to the incident light and at 350 nm wavelength for various F-actin/ $\alpha$ -actinin solutions. Results from measurements using 3  $\mu$ M F-actin at a molar ratio to  $\alpha$ -actinin,  $r_{A\alpha}$  4:1 are shown in Fig. 2. Since linear temperature increases from 6°C and 25°C over 14 and 120 min showed huge inten-

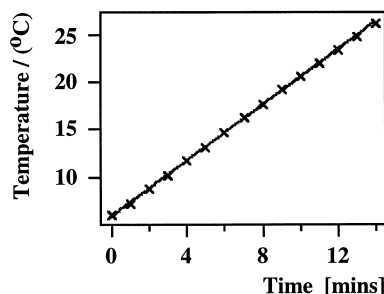


Fig. 1. Determination of the heating rate of a 1 ml F-buffer solution in a quartz cuvette. The temperature is maintained ( $\pm 0.1^\circ\text{C}$ ) by an external heater and an electronically controlled sensor in the cell. Slope of the computer fitted line is 2°C/min. Note: the data points represent an average of three separate experiments.

sity ( $I$ ) increases and similar curve structure, indicating that the F-actin/ $\alpha$ -actinin solution had reached equilibrium at every temperature, all subsequent measurements were performed over a period of 14 min. Pure F-actin and  $\alpha$ -actinin used as control exhibited no intensity changes, ( $I$ ) above the baseline noise for the entire temperature range (data not shown).

The temperature-dependent light scatter intensity ( $I$ ) was examined at different experimental conditions to demonstrate the universality of  $\Delta H$  and  $K_0$ . In the first set of experiments various molar ratios of F-actin to  $\alpha$ -actinin were used. With increasing  $\alpha$ -actinin [ $\alpha$ ] an augmentation of the maximal light intensity ( $I$ ) and a shift of the gel-sol transition point  $T_g$  to higher temperatures was observed (Fig. 3). This behavior is expected as the equilibrium constant  $K$  represents the relation of  $[C]/([A][\alpha])$  (Eq. 1a, Eq. 1b). Higher  $\alpha$ -actinin [ $\alpha$ ] should lead at constant F-actin [ $A$ ] to increased network formation [ $C$ ], and assuming that the degree of cross-linking is proportional to the light scatter intensity (Eq. 5), the relation of  $\alpha$ -actinin [ $\alpha$ ] as well as the absolute intensity,  $I(T)$  should be linear. Plotting these variables against F-actin/ $\alpha$ -actinin molar ratios confirms these assumptions (Table 1A–C). Tempel et al. [11] observed a similar temperature-dependent behavior at various molar ratios  $r_{A\alpha}$  and explained this kinetically by a displacement law,  $r_{A\alpha}/T_g \approx \text{const}$ . These authors pointed out

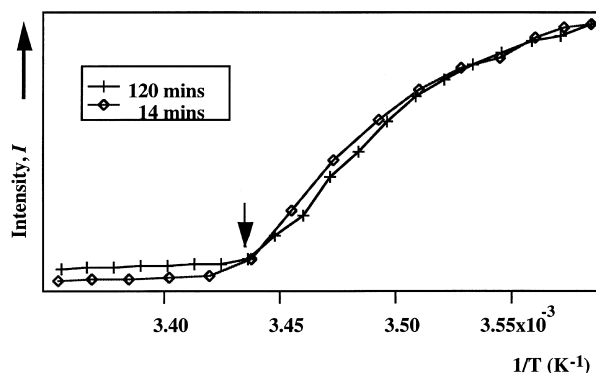


Fig. 2. Linear temperature increase from 6–25°C at 120 min (+) and 14 min (o) duration. Conditions: 3  $\mu$ M F-actin at a molar ratio to  $\alpha$ -actinin, 4:1; light scattering at 350 nm and 90° angle. The arrow indicates the end of the actin network formation. Note: linear temperature decreases from 25–6°C showed identical curve structure, and pure F-actin showed insignificant intensity changes over this temperature range (data not shown).

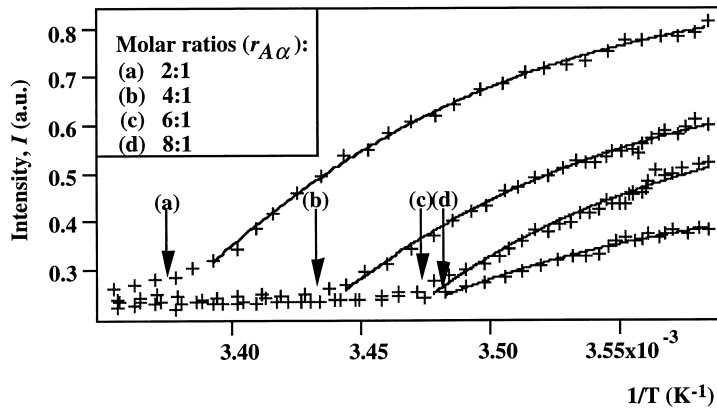


Fig. 3. Linear temperature increase from 6–25°C at various molar ratios of F-actin to  $\alpha$ -actinin,  $r_{A\alpha}$ . Conditions: 3  $\mu$ M F-actin; light scattering at 350 nm, at 90° angle, and 14 min duration. The arrows indicate the end of the actin network formation.

that the ‘characteristic’ length of entanglement is responsible and not the mesh size of networks. This encouraged us to examine the influence of F-actin filament length on the gel-sol transition point  $T_g$ . Using F-actin in the presence of gelsolin at a molar ratio,  $r_{AG}$ , of 2000:1, and maintaining the F-actin filament length constant at 5–6  $\mu$ m [20] compared to random lengths distribution ( $\leq 50$  nm; [21]), had a significant influence on  $(I)T$  and  $T_g$  (Fig. 4a). Similar behavior was observed when we varied the F-actin concentration (Fig. 4b). Increasing the F-actin concentration from 3  $\mu$ M to 6  $\mu$ M shifted  $T_g$  to higher temperatures by a factor of  $\sim 1.3$ . Tempel et al. [11] suggested that this phenomenon can be explained by (Eq. 4). Since the temperature of the reaction with  $p_\alpha(T) = 1/2$  is determined by  $[A]K_0 \exp(\Delta H/RT) = 1$  with  $\Delta H \approx RT$ , an increase of  $[A]$  would also increase  $T_g$ . Grazi et al. [22] described this behavior as follows: the temperature-dependent dissociation of  $\alpha$ -actinin from the F-actin/ $\alpha$ -actinin bundle complex results in a ‘quasi-parallel’ filament arrangement. The reason for this phenomenon is probably the reduced flexibility of the long, interchained actin polymers. Note: in control measurements, testing the temperature-dependent cross-linking of filamin with 3  $\mu$ M F-actin at various molar ratios to

filamin, we detected no changes in light scatter intensity  $(I)T$ , indicating that  $\alpha$ -actinin has a special function among F-actin cross-linking proteins (data not shown).

Further, Tempel et al. [11] observed with different temperatures when measuring creep  $J(t)$  that gels almost reached equilibrium at  $t \sim 10^4$  s, exhibiting a small finite slope. This behavior was attributed to the *off*-rates of F-actin/ $\alpha$ -actinin complexes. We have measured the *off*- and *on*-rates in previous stopped flow experiments ([8,10] and unpublished results). The *off*- and *on*-rates decreased linearly by a factor of 200 and 20, varying between  $\sim 10$  s $^{-1}$  and  $\sim 0.05$  s $^{-1}$ , and  $\sim 4 \times 10^6$  M $^{-1}$  s $^{-1}$  and  $\sim 2 \times 10^5$  M $^{-1}$  s $^{-1}$ , at 25°C and 5°C, respectively (Table 2), confirming these authors’ assumption [11].

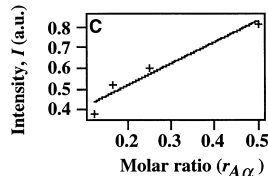
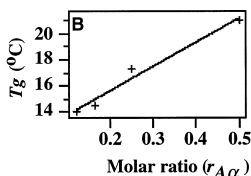
To analyze the light scatter intensity  $(I)T$  with differences in temperature we divided the trace into three regions: (i) plateau, (ii) slope, and (iii) ascendancy. The sum of the light scatter intensity given in arbitrary units (a.u.) for the plateau region (i) can be compared with pure F-actin or the unbound state of  $\alpha$ -actinin [23]. Grazi et al. [24] described this temperature range ‘where actin filaments have undergone only minimal binding with  $\alpha$ -actinin’ and Tempel et al. [11] observed within this temperature range ‘a homogeneously distributed gel’. The intensity change  $(I)T$  observed for region (ii) may be regarded as ‘transitional’ at increased binding activity due to the rise in affinity (Table 2) and depending on where cross-linking takes place [11] or where ‘moderate bundling of actin filaments of single-bound  $\alpha$ -actinin occurs’ [24]. The significant rise in light scatter intensity  $(I)T$  in region (iii) is probably due to the dramatic increase in affinity of  $\alpha$ -actinin with F-actin activity or ‘double-bound  $\alpha$ -actinin into tightly bunched actin filaments’ [24] as well as the consequent inhomogeneity of the actin filament network and sol-gel transition [11]. In our analyses, we fitted region (iii) for various F-actin/ $\alpha$ -actinin solutions and molar ratios  $r_{A\alpha}$  using (Eq. 4).

$$I(T) \propto \frac{1}{2} \frac{[A]K_0 \exp(\Delta H/RT)}{[A]K_0 \exp(\Delta H/RT) + 1}$$

This equation allowed us to determine the heat of the association,  $\Delta H$ , and the proportionality constant,  $K_0$ . The calculated mean value for the different molar ratios,  $r_{A\alpha}$ , which varied insignificantly, indicated for  $\Delta H = 84.2(\pm 0.18)$  kJ mol $^{-1}$  and  $K_0 = 5.9(\pm 0.27) \times 10^{-10}$  mol $^{-1}$ . These constants were then inserted into (Eq. 3), determining the equilibrium

Table 1  
(A) Temperature-dependent gel points  $T_g$  and absolute intensities  $(I)T$ , at various actin/ $\alpha$ -actinin molar ratios  $r_{A\alpha}$ , ( $T_g^{-1}$ ;  $10^{-3}$  K $^{-1}$ : 3.401 at 2:1; 3.444 at 4:1; 3.478 at 6:1; 3.483 at 8:1), and plots of gel points  $T_g$  (B), and absolute intensity,  $I$  (C), respectively. Data taken from traces in Fig. 3 show linear dependence.

Molar ratio ( $r_{A\alpha}$ )	2:1	4:1	6:1	8:1
$T_g$ (°C)	21.0	17.3	14.5	14.1
Intensity, $I$	0.81	0.60	0.52	0.38



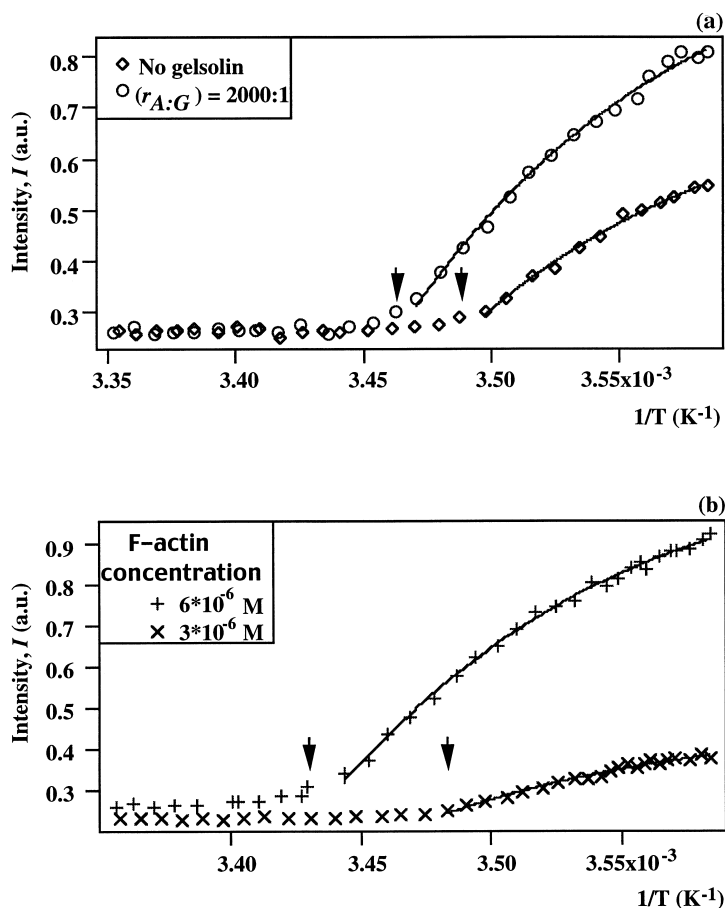


Fig. 4. Linear temperature increase from 6–25°C in 14 min, at F-actin/ $\alpha$ -actinin at molar ratio  $r_{A\alpha}$  8:1 (a) in the absence and presence of gelsolin, of  $r_{AG}$  2000:1 and (b) at different F-actin concentrations. The arrows indicate the end of the actin network formation. Conditions as in Fig. 3.

constant, for various temperatures. The calculated values agree markedly well with published results [8–10] and recently generated stopped flow data (Table 2), indicating that the

kinetic approach of the percolation theory can be used to predict the equilibrium constant  $K$  in temperature-dependent cross-linking processes.

Table 2

Temperature-dependent, measured (stopped flow), and calculated equilibrium constants  $K$

Temperature (°C)	$(K_{eq} = k_{on}/k_{off})$	Measured $K$ ( $\times 10^6$ M <sup>-1</sup> )	Calculated $K$ ( $\times 10^6$ M <sup>-1</sup> )
5	$k_{on} = 2.0 \times 10^5$ M <sup>-1</sup> s <sup>-1</sup> (1b) $= 2.2 \times 10^5$ M <sup>-1</sup> s <sup>-1</sup> (2)	4.4	3.9
7	$k_{off} = 0.05$ s <sup>-1</sup> (2); $< 0.5$ s <sup>-1</sup> (1b) $k_{on} = 5.0 \times 10^5$ M <sup>-1</sup> s <sup>-1</sup> (3)	3.3	3.4
15	$k_{off} = 0.15$ s <sup>-1</sup> (3) $k_{on} = 1.8 \times 10^6$ M <sup>-1</sup> s <sup>-1</sup> (1a) $= 1.4 \times 10^6$ M <sup>-1</sup> s <sup>-1</sup> (1b) $= 3.0 \times 10^6$ M <sup>-1</sup> s <sup>-1</sup> (2)	1.2; 1.6; 1.4	1.12
20	$k_{off} = 1.5$ s <sup>-1</sup> (1a) $= 0.8$ s <sup>-1</sup> (1b) $= 2.2$ s <sup>-1</sup> (2) $k_{on} = 2.0 \times 10^6$ M <sup>-1</sup> s <sup>-1</sup> (2) $= 1.0 \times 10^6$ M <sup>-1</sup> s <sup>-1</sup> (4)	0.87; 2.5	0.62
25	$k_{off} = 2.3$ s <sup>-1</sup> (2) $= 0.4$ s <sup>-1</sup> (4) $k_{on} = 4.0 \times 10^6$ M <sup>-1</sup> s <sup>-1</sup> (1a) $= 2.2 \times 10^6$ M <sup>-1</sup> s <sup>-1</sup> (2) $k_{off} = 9.6$ s <sup>-1</sup> (1a) $= 10.0$ s <sup>-1</sup> (2)	0.22; 0.42	0.34

(1a, b) These researchers examined the binding of  $\alpha$ -actinin (fragment) to F-actin [30,9]; (2) unpublished transient data from this laboratory under conditions used by Tempel et al. [11]; (3) to compare data from other labs, all traces were fitted to a single exponential, thus the authors are aware of biphasic interactions between F-actin and  $\alpha$ -actinin cf. [10]; (4) [8].

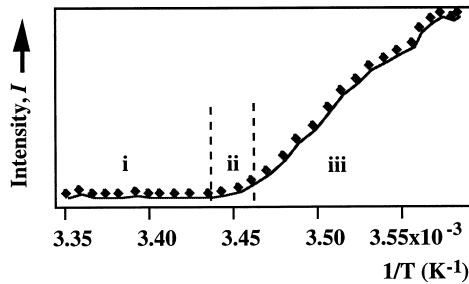


Fig. 5. Various temperature-dependent stages of light scatter intensity ( $I/T$ ) of F-actin/ $\alpha$ -actinin binding at a molar ratio  $r_{A\alpha}$  4:1; i, plateau; ii, slope; and iii, ascendancy. Conditions as in Fig. 3.

#### 4. Discussion

Ever since Stossel et al. [25] proposed that  $\alpha$ -actinin plays an active role in remodeling the actin cytoskeleton by controlling the existence and extent of cross-linking, a proposal that has far-reaching implications for cellular regulation and motility, research has been substantial in response [5,26]. Various models have been introduced in an attempt to gain insight into the subtle processes which govern cellular regulation and motility: cellular automaton [23], cellular tensegrity [27], and percolation [11,28].

In this work, we describe the properties of the interaction of actin filaments with the regulatory proteins,  $\alpha$ -actinin and gelsolin, in a concentration and temperature-dependent manner. Our data, based on the kinetic approach of the percolation model described by Tempel et al. [11], capture a linear relationship of the gel-sol transition point,  $T_g$ , and light intensity, ( $I/T$ ), of actin filaments bound to  $\alpha$ -actinin at various molar ratios  $r_{A\alpha}$ . With increasing actin/ $\alpha$ -actinin molar ratios and F-actin concentrations,  $T_g$  is shifted to higher temperatures, which is probably due to spatial hindrance [24] and to decreasing affinity of the F-actin to  $\alpha$ -actinin [22]. Similarly, the binding affinity of the actin/ $\alpha$ -actinin complex shows with changes in temperature a linear dependence of the equilibrium constant  $K$  (Fig. 5, region iii). The presence of gelsolin,  $r_{AG}$  of 2000:1, and different amounts of F-actin also change  $T_g$  to higher temperatures, indicating that the cross-linking/bundling behavior is affected by actin filament lengths and F-actin concentration.

From these findings it can be concluded that (i) the activity of  $\alpha$ -actinin is directly influenced by temperature, and that (ii) the effect resulting from the change in temperature is proportional to changes in the concentration of  $\alpha$ -actinin at constant temperature i.e. (iii) temperature-dependent measurements are equivalent to concentration-dependent measurements. Sackmann [29] explained this phenomenon in terms of *microgel* formation, which is the result of chemical cross-linking processes and is equivalent to additional forces between filaments. At sufficiently high cross-linker ratio and electrostatic attraction between filaments, microscopic spinodal phase separation occurs, forming areas of high and low polymer concentration.

Tempel et al. [11] observed in their rheological study that at cross-linker concentrations  $r_{A\alpha} \geq 55$  and at temperatures  $T < 10^\circ\text{C}$  *microgels* are formed, and that at higher cross-linker concentration in this temperature range macroscopic network formation of filament bundles occurs.

Finally, since there is growing evidence that the mechanical integrity of the cytoskeleton largely consists of a three-dimensional interconnected protein mesh and that these fibrous units provide the mechanical links that are crucial for cell movement, form, and viscoelasticity, the approach of percolation may also be used to explain cellular events [30].

*Acknowledgements:* We thank Hulda Kirpal for protein purification, Klaus Kroy for valuable discussions, and Judith Feldmann and Elizabeth Nicholson for careful reading of the manuscript. This work was supported by the American Cancer Society, Deutsche Forschungsgemeinschaft, and North Atlantic Treaty Organization.

#### References

- [1] Isenberg, G. (1996) *Sem. Cell Dev. Biol.* 7, 707–715.
- [2] Isenberg, G. and Niggli, V. (1998) *Int. Rev. Cytol.* 178, 73–125.
- [3] Jockusch, B.M. et al. (1995) *Annu. Rev. Cell Dev. Biol.* 11, 379–416.
- [4] Bennett, J.P., Zaner, K.S. and Stossel, T.P. (1984) *Biochemistry* 23, 5081–5086.
- [5] Sato, M., Schwartz, W.H. and Pollard, T.D. (1987) *Nature* 325, 828–830.
- [6] Wachsstock, D.H., Schwartz, W.H. and Pollard, T.D. (1993) *Biophys. J.* 65, 205–214.
- [7] Senger, R. and Goldmann, W.H. (1995) *Biochem. Mol. Biol. Int.* 35, 103–109.
- [8] Goldmann, W.H. and Isenberg, G. (1993) *FEBS Lett.* 336, 408–410.
- [9] Kuhlman, P.A. et al. (1994) *FEBS Lett.* 339, 297–301.
- [10] Goldmann, W.H. et al. (1998) in: G. Isenberg (Ed.), *Modern Optics, Electronics and High Precision Techniques in Cell Biology*, Springer Verlag, Heidelberg, pp. 160–171.
- [11] Tempel, M., Isenberg, G. and Sackmann, E. (1996) *Phys. Rev. E* 54, 1802–1810.
- [12] Craig, S.W., Lancashire, C.L. and Cooper, J.A. (1982) *Methods Enzymol.* 85, 316–330.
- [13] Laemmli, U. (1970) *Nature* 227, 680–685.
- [14] Spudich, J.A. and Watt, S. (1971) *J. Biol. Chem.* 246, 4866–4871.
- [15] Cooper, J.A. et al. (1987) *J. Cell Biol.* 104, 491–501.
- [16] Bradford, M.M. (1976) *Anal. Biochem.* 72, 248–254.
- [17] de Gennes, P.G. (1979) *Scaling Concepts in Polymer Physics*, Cornell University Press, Ithaca, NY.
- [18] Goetter, R. et al. (1995) *Macromolecules* 29, 30–36.
- [19] Kroy, K. and Frey, E. (1997) *Phys. Rev. E* 55, 3092–3101.
- [20] Coppin, C.M. and Leavis, P.C. (1992) *Biophys. J.* 63, 794–807.
- [21] Kaes, J. et al. (1996) *Biophys. J.* 70, 609–625.
- [22] Grazi, E. et al. (1994) *Biochem. J.* 298, 129–133.
- [23] Dufort, P.A. and Lumsden, C.J. (1993) *Cell Motil. Cytoskelet.* 25, 87–104.
- [24] Grazi, E. et al. (1993) *Biochemistry* 32, 8896–8901.
- [25] Stossel, T.P. et al. (1985) in: G. Palade, B. Alberts and J. Spudich (Eds.), *Annu. Rev. Cell Biol., Annu. Rev. Inc.*, Palo Alto, CA, pp. 353–402.
- [26] Janmey, P.A. et al. (1990) *Nature* 345, 89–92.
- [27] Ingber, D.E. et al. (1994) *Int. Rev. Cytol.* 150, 173–224.
- [28] Forgacs, G. (1995) *J. Cell Sci.* 108, 2131–2143.
- [29] Sackmann, E. (1994) *Macromol. Chem. Phys.* 194, 7–28.
- [30] Xu, J., Wirtz, D. and Pollard, T.D. (1998) *J. Biol. Chem.* 273, in press.